HHS Public Access

Author manuscript

Radiology. Author manuscript; available in PMC 2024 January 01.

Published in final edited form as:

Radiology. 2023 January ; 306(1): 279–287. doi:10.1148/radiol.220158.

Prospective Evaluation of Immune Activation Associated with Response to Radioembolization Assessed with PET/CT in Women with Breast Cancer Liver Metastasis

Amy R. Deipolyi, MD, PhD,
Department of Surgery, West Virginia University/Charleston Division, Charleston Area Medical Center, 3200 MacCorkle Ave SE, Charleston, WV 25304

C. Bryce Johnson, MD, PhD,
Department of Radiation Oncology, Inova Schar Cancer Institute, Fairfax, Va

Christopher C. Riedl, MD, PhD,
imagingwest, Hawthorne, NY

Henry Kunin, BA,
Interventional Radiology Service, Memorial Sloan-Kettering Cancer Center, New York, NY

Stephen B. Solomon, MD,
Interventional Radiology Service, Memorial Sloan-Kettering Cancer Center, New York, NY

Rahmi Oklu, MD, PhD,
Vascular & Interventional Radiology, Laboratory for Patient Inspired Engineering, Mayo Clinic, Scottsdale, Ariz

Meier Hsu, MS,
Department of Epidemiology and Biostatistics, Memorial Sloan-Kettering Cancer Center, New York, NY

Chaya S. Moskowitz, PhD,
Department of Epidemiology and Biostatistics, Memorial Sloan-Kettering Cancer Center, New York, NY

Faruk E. Kombak, MD,
Department of Pathology, Precision Pathology Center, Memorial Sloan-Kettering Cancer Center, New York, NY

Address correspondence to A.R.D. (amy.deipolyi@camc.org).

Author contributions: Guarantors of integrity of entire study, **A.R.D., C.B.J.**; study concepts/study design or data acquisition or data analysis/interpretation, all authors; manuscript drafting or manuscript revision for important intellectual content, all authors; approval of final version of submitted manuscript, all authors; agrees to ensure any questions related to the work are appropriately resolved, all authors; literature research, **A.R.D., C.B.J., F.E.K., J.P.E.**; clinical studies, **A.R.D., C.C.R., H.K.**; experimental studies, **A.R.D., C.B.J., R.O., F.E.K., U.B.**; statistical analysis, **M.H., C.S.M., J.P.E.**; and manuscript editing, **A.R.D., C.B.J., S.B.S., R.O., M.H., C.S.M., F.E.K., J.P.E.**

Disclosures of conflicts of interest: A.R.D. No relevant relationships. **C.B.J.** No relevant relationships. **C.C.R.** No relevant relationships. **H.K.** No relevant relationships. **S.B.S.** Consulting fees from Varian and Advantagene; research grants from GE Healthcare, AngioDynamics, and Johnson & Johnson. **R.O.** No relevant relationships. **M.H.** No relevant relationships. **C.S.M.** Payment or honoraria for lectures or presentations from the RSNA. **F.E.K.** No relevant relationships. **U.B.** No relevant relationships. **J.P.E.** Consulting fees from AstraZeneca.

Umesh Bhanot, MD, PhD,
Department of Pathology, Precision Pathology Center, Memorial Sloan-Kettering Cancer Center, New York, NY

Joseph P. Erinjeri, MD, PhD
Interventional Radiology Service, Memorial Sloan-Kettering Cancer Center, New York, NY

Abstract

Background: The impact of transarterial radioembolization (TARE) of breast cancer liver metastasis (BCLM) on antitumor immunity is unknown, which hinders the optimal selection of candidates for TARE.

Purpose: To determine whether response to TARE at PET/CT in participants with BCLM is associated with specific immune markers (cytokines and immune cell populations).

Materials and Methods: This prospective pilot study enrolled 23 women with BCLM who planned to undergo TARE (June 2018 to February 2020). Peripheral blood and liver tumor biopsies were collected at baseline and 1–2 months after TARE. Monocyte, myeloidderived suppressor cell (MDSC), interleukin (IL), and tumor-infiltrating lymphocyte (TIL) levels were assessed with use of gene expression studies and flow cytometry, and immune checkpoint and cell surface marker levels with immunohistochemistry. Modified PET Response Criteria in Solid Tumors was used to determine complete response (CR) in treated tissue. After log-transformation, immune marker levels before and after TARE were compared using paired *t* tests. Association with CR was assessed with Wilcoxon rank-sum or unpaired *t* tests.

Results: Twenty women were included. After TARE, peripheral IL-6 (geometric mean, 1.0 vs 1.6 pg/mL; $P = .02$), IL-10 (0.2 vs 0.4 pg/mL; $P = .001$), and IL-15 (1.9 vs 2.4 pg/mL; $P = .01$) increased. In biopsy tissue, lymphocyte activation gene 3–positive CD4+ TILs (15% vs 31%; $P < .001$) increased. Eight of 20 participants (40% [exact 95% CI: 19, 64]) achieved CR. Participants with CR had lower baseline peripheral monocytes (10% vs 29%; $P < .001$) and MDSCs (1% vs 5%; $P < .001$) and higher programmed cell death protein (PD) 1–positive CD4+ TILs (59% vs 26%; $P = .006$) at flow cytometry and higher PD-11 staining in tumor (2% vs 1%; $P = .046$).

Conclusion: Complete response to transarterial radioembolization was associated with lower baseline cytokine, monocyte, and myeloid-derived suppressor cell levels and higher programmed cell death protein 1–positive tumor-infiltrating lymphocyte levels.

Summary

Immune markers, including interleukin (IL) 6, IL-10, monocytes, myeloid-derived suppressor cells, and programmed cell death protein 1–positive CD41 tumor infiltrating lymphocytes, were associated with response to radioembolization of breast cancer liver metastasis as evaluated at PET/CT.

Yttrium 90 transarterial radioembolization (TARE) is an emerging therapy for the treatment of breast cancer liver metastasis (BCLM). TARE for BCLM is primarily used to treat multifocal refractory hepatic disease in the context of liver-only progression to maintain patients on one line of systemic therapy, and previous retrospective research suggests that TARE is associated with better imaging outcomes and reduced toxicity compared with

chemoembolization (1). While over 70% of patients with breast cancer achieve metabolic imaging response to TARE and early imaging response is associated with prolonged survival (2,3), there are limitations to its efficacy. First, there are no reliable indicators that predict which patients will achieve radiographic response or survive longer after TARE (1,3). Second, response lasts for a median of 6 months, but most patients then develop hepatic progression (2). Finally, treatment of hepatic tumors has no impact on extrahepatic metastasis.

One strategy to address these limitations is to explore the potential of TARE to induce local and systemic antitumor immunity. TARE is anticipated to induce immune response because it delivers high-dose radiation at a low dose rate, and previous studies on external radiation suggest that greater immune response is associated with higher dose radiation to liver tumors given over multiple fractions (4). The efficacy of external radiation requires intact immunity (5), suggesting that immune markers (ie, levels of cytokines, as well as presence and levels of immune cell types) may predict response to TARE. TARE for hepatocellular carcinoma induces immune response (6), like external radiation (7). By defining the antitumor immune response to TARE performed for BCLM, immunotherapy targets for potential combination treatments may be suggested to increase and prolong the efficacy of TARE and potentially induce immune-mediated extrahepatic response by abscopal effects. The purpose of our study was to evaluate changes in immune marker levels after TARE performed to treat BCLM. The hypothesis was that metabolic imaging response to TARE is associated with immune markers.

Materials and Methods

Study Design

Participants with breast cancer with liver-dominant bilobar progression provided informed consent to enroll in this prospective single-center pilot study compliant with the Health Insurance Portability and Accountability Act and approved by the institutional review board (Table 1, Fig 1). TARE was offered for liver-only progression despite systemic therapy (Table 2). Participants underwent baseline peripheral blood collection and liver tumor biopsy during the mapping procedure or immediately preceding the first lobar TARE. Post-TARE peripheral blood collection and biopsy of a radioembolized tumor were performed 4–8 weeks later, immediately before the second lobar TARE. Participants underwent baseline PET/CT within 1 month of mapping. Two to 3 months following first lobar TARE, PET/CT was performed to assess imaging response.

The trial was closed after 23 participants were recruited (June 2018 to February 2020) based on a power analysis to detect differences in response for phosphoinositide 3–kinase (PI3K) pathway variants (3). Two participants who underwent baseline specimen collection during mapping were excluded from analysis due to extrahepatic progression precluding TARE. One participant underwent one lobar TARE; based on biopsy results, she initiated different systemic therapy and thus dropped out of the study. Therefore, 20 women (mean age, 58 years ± 11 [SD]), were included for analysis, including two with triple-negative breast cancer.

Imaging

Participants fasted for 4 or more hours before intravenous fluorine 18 fluorodeoxyglucose injection (444–555 MBq), when plasma glucose measured less than 200 mg/dL. After injection, patients rested for 60 minutes before undergoing PET/CT. Images were acquired on GE Healthcare Discovery PET/CT systems, with patients in the supine position, from midskull to midthigh with 3-minute acquisitions per bed position. Companion noncontrast CT scans were obtained.

Procedures

Sequential lobar TARE was performed using glass microspheres (TheraSpheres, Boston Scientific), targeting 120 Gy by using the medical internal radiation dosimetry model, with an average of 3219 MBq ± 1147 (SD) (range, 1739–5883 MBq) administered during the first treatment. Immediately before infusion, peripheral blood was collected and image-guided coaxial core tumor biopsy performed with 17-gauge introducers. The largest, most peripheral biopsy target was selected from the lobe planned to be treated in the first administration; at least two cores measuring 2 cm were collected near the tumor periphery with TEMNO (Merit Medical) or Bard Mission (BD) coaxial systems.

Flow Cytometry and Cytokine Analysis

Peripheral blood mononuclear cells and tumor tissue were analyzed in T-cell flow cytometry panels to evaluate activation and exhaustive phenotypes. Samples were thawed and stained with fixable aqua viability dye (Invitrogen) and surface marker antibodies (Table E1 [online]). Cells were fixed, permeabilized, and stained intracellularly. Stained cells were acquired on BD Biosciences LSRFortessa and analyzed using FlowJo (BD). CD14+HLA-DR^{lo} monocytic myeloid-derived suppressor cell (MDSC) frequencies were derived by gating on live, lineage-negative CD14+ monocytes and exporting this population to a computational algorithm (8). Specimens were considered sufficient for analysis when more than 30 tumor-infiltrating lymphocytes (TILs) were detected by the instrument.

Frozen plasma samples were thawed, centrifuged, and diluted for cytokine analysis. Cytokines were quantitated with V-PLEX Human Proinflammatory Panel 10-plex kits (Meso Scale Diagnostics), and data were analyzed using Discovery Workbench (Meso Scale Diagnostics).

Assays of Tissue Fixed in Formalin and Embedded in Paraffin

Genomic DNA was extracted in the Pathology Department’s molecular diagnostic laboratory from baseline biopsy specimens. MSK-IMPACT, or Memorial Sloan-Kettering–Integrated Mutation Profiling of Actionable Cancer Targets, a high-throughput hybridization capture-based next-generation sequencing assay using a 468-gene oncopanel (9), was used for genotyping to categorize participants with or without PI3K pathway variations (3).

For hematoxylin and eosin staining and immunohistochemistry, 4-μm slices were obtained. Immunohistochemistry was performed on the Bond-Rx platform with use of standard immunoperoxidase methods (Table E1 [online]). Two pathologists (F.E.K. and U.B., with 10 and 20 years of experience, respectively) reviewed slides under light microscopes. The

percent viable tumor and presence of tumor stroma were assessed on hematoxylin and eosin–stained slices. For CD4, CD8, CD14, lymphocyte activation gene 3 (LAG3), and programmed cell death protein (PD) 1, the percent area occupied by positive mononuclear inflammatory cells of the total stromal area within the borders of the invasive tumor was calculated (10). For programmed death ligand 1, the Combined Positive Score was implemented (11).

RNA was extracted from tissue fixed in formalin and was analyzed on the NanoString nCounter system with use of the PanCancer IO 360 Panel (Canopy Biosciences). Raw data counts were normalized using the geometric mean of 20 housekeeping genes in the IO360 Panel and then log-transformed (2). IO360 gene analysis for 48 signatures measuring immune cell abundance, immune signaling, and tumor and stromal biologic characteristics was performed (12,13).

Imaging Analysis

Pre-TARE liver tumor burden was calculated at CT or MRI with use of TeraRecon (TeraRecon) as the percentage of liver parenchyma occupied by the tumor. Regions of interest were drawn on baseline contrast-enhanced anatomic images when available; noncontrast CT regions of interest were drawn during review of concurrent PET images to ensure all tumors were identified. Regions of interest were confirmed by an experienced radiologist blinded to other study outcomes (A.R.D., with 5 years of experience). Modified PET Response Criteria in Solid Tumors was used to assess imaging response for each hepatic area targeted by TARE (14,15). The maximum standardized uptake value (SUV_{max}) was measured by a nuclear medicine fellowship–trained diagnostic radiologist (C.C.R., with 10 years of experience) blinded to other study outcomes. SUV_{max} was normalized by subtracting the average standardized uptake value of uninvolved liver parenchyma. Complete response (CR) was defined as at least 80% normalized SUV_{max} (16). Participants were categorized as achieving CR or as nonresponders (not achieving CR). The four participants who died before second lobar TARE were considered nonresponders.

Statistical Analysis

Clinical characteristics were summarized as medians with IQRs or means ± SDs for continuous variables and frequencies with percentages for categorical variables. Responders and nonresponders were compared using Wilcoxon rank-sum and Fisher exact tests for continuous and categorical variables, respectively. For flow cytometry analysis, values below the limit of detection were imputed assuming censored normal distributions or by substitution with half the detection limit value when censoring was lighter (<20%) (17). No imputation was performed for missing data. Pre- and post-TARE marker levels were summarized with geometric means and geometric SD factors. Differences were characterized as the ratio of the geometric means. Changes in marker values from pre- to post-TARE were assessed using paired *t* tests and compared between responders and nonresponders using Welch two-sample *t* tests, with data transformed using a natural log transformation. Associations of baseline marker values with CR were evaluated using two-sample *t* tests. Due to the small number of available data, baseline immunohistochemistry data were summarized as medians with IQRs and evaluated for association with CR with use

of Wilcoxon rank-sum tests. Analyses were performed using R version 4.1.2 (R Foundation for Statistical Computing). $P < .05$ was considered indicative of statistically significant difference.

Results

Participant Characteristics

Among 20 participants with pre-TARE imaging, mean baseline tumor burden was 22% ± 17 (SD), and mean normalized SUV_{max} was 9 ± 5. Sixteen participants had pre- and post-TARE PET/CT images, acquired 32 days ± 23 before and 73 days ± 21 after TARE. Four participants died during the study period and were classified as nonresponders. Mean change in SUV_{max} was −68% ± 41 in hepatic tumors targeted during the first lobar TARE among the 17 participants with pre- and post-TARE metabolic imaging. Eight of 20 participants (40%; exact 95% CI: 19, 64) achieved CR in the first treated hepatic lobe. Characteristics of participants who achieved CR compared with those who did not (nonresponders) are summarized in Table 1. There was no evidence of a difference between the two response groups regarding hormone receptor status, tumor burden, pre-TARE SUV_{max}, lung shunt fraction, or activity of administered microspheres. Among the 20 patients, 18 died during follow-up. The follow-up time for the two survivors was 3.3 months and 20.9 months. Median overall survival for all participants was 6.3 months (95% CI: 4.3, 14).

Peripheral Blood

There were 20 participants with baseline blood specimens; 17 had blood drawn after TARE. Among participants with available pre- and post-TARE specimens (Table E2 [online]), TARE was associated with increased peripheral IL-6 (1.0 vs 1.6 pg/mL; $P = .02$), IL-10 (0.2 vs 0.4 pg/mL; $P = .001$), and IL-15 (1.9 vs 2.4 pg/mL; $P = .01$). No consistent changes in monocytes or MDSCs were observed (Table 3).

Among 20 participants who had blood drawn at baseline, eight had CR according to the modified PET Response Criteria in Solid Tumors and 12 did not. Among the 17 participants with peripheral blood drawn after TARE, eight achieved CR and nine did not. Participants with CR, compared with nonresponders, had lower baseline peripheral levels of IL-6 (0.5 vs 1.8 pg/mL; $P = .04$), IL-10 (0.2 vs 0.3 pg/mL; $P = .04$), monocytes (10% vs 29%; $P < .001$), and MDSCs (1% vs 5%; $P < .001$) (Table 4, Fig 2).

Participants with CR and nonresponders were compared regarding changes in peripheral markers before and after TARE. IL-8 levels decreased in responders and increased in nonresponders, although the difference was not significant (mean difference, 0.9 vs 1.4 pg/mL; $P = .07$).

Biopsy Tissue

There were 20 participants with biopsy tissue collected at baseline, and 14 of these participants had biopsy tissue collected after TARE. Of 20 participants with pre-TARE biopsy tissue, 19 had sufficient events for analysis of TILs. Of 14 participants with post-TARE biopsy tissue, 12 had sufficient events for analysis of TILs. Of 19 participants with

sufficient pre-TARE biopsy tissue, eight achieved CR and 11 did not. Of 12 participants with sufficient post-TARE biopsy tissue, five achieved CR and seven did not. Participants with CR, compared with nonresponders, had higher PD-1+ CD4+ TILs (59% vs 26%; $P = .006$) at baseline (Fig 2). Among all participants with available pre- and post-TARE specimens, mean increase was observed in LAG3+ CD4+ TILs (15% vs 31%; $P < .001$) (Table 3). Complete responders were compared with nonresponders regarding changes in TILs in biopsy tissue before and after TARE. CD8+/CD4+ regulatory T-cell ratios were increased in responders and decreased in nonresponders, although the difference was not significant (mean difference, 0.5 vs −0.9; $P = .06$).

Six participants (three complete responders and three nonresponders) had sufficient pre- and post-TARE biopsy tissue for RNA expression analysis. Comparing pre- and posttreatment samples, a 1.7-fold increase was observed in nitric oxide synthase 2 expression after treatment (unadjusted $P = .04$), and a 1.7-fold decrease was observed in the expression signature for mast cells (unadjusted $P = .04$). There were too few participants to identify significant differences between response groups.

Twenty participants underwent response assessment and had pre-TARE biopsy tissue available for MSK-IMPACT testing. Eight participants were found to have PI3K pathway variations, and 12 were wild type. There was no evidence of a difference in imaging response between participants with variant or wild-type PI3K (two of eight participants [25%] vs six of 12 [50%]; $P = .37$).

Fourteen participants had sufficient pre-TARE tissue for PD-1 and programmed death ligand 1 immunohistochemistry analysis, including six nonresponders and eight responders. Only five of these (two nonresponders and three responders) had sufficient post-TARE tissue for PD-1 and programmed death ligand 1 analysis. There were 11 participants with sufficient pre-TARE tissue for CD4, CD8, CD14, and LAG3 immunohistochemistry analysis, including five nonresponders and six responders. Only four of these (two responders and two nonresponders) had sufficient post-TARE tissue for CD4, CD8, CD14, and LAG3 analysis. Because of the low numbers of participants with sufficient post-TARE tissue, only baseline levels of markers were compared. CR was associated with higher median levels of pre-TARE PD-1 levels (2% vs 1%; $P = .046$) (Table 4, Fig 3).

Discussion

This study on the immunologic effects of transarterial radioembolization (TARE) performed for breast cancer liver metastasis revealed two major findings. First, peripherally, response to TARE was associated with increased interleukin (IL) 6, IL-10, and IL-15, and, in the tumor microenvironment, with increased lymphocyte activation gene 3–positive CD4+ tumor-infiltrating lymphocyte (TILs) and nitric oxide synthase 2 expression and decreased mast cell levels. Second, lower baseline peripheral IL-6, IL-10, and immunosuppressive myeloid-derived suppressor cells and monocytes and higher programmed cell death protein 1–positive CD4+ TILs in the tumor microenvironment were associated with response to TARE.

Our findings complement the existing literature on the immunologic effects of image-guided therapy for other cancers. Thermal ablation of melanoma increases IL-6 and IL-10 levels (18), suggesting that ablation can induce immunosuppressive effects. For embolotherapies, particle size and type impact the extent of inflammatory cell infiltrates and intratumoral lymphocyte accumulation (19–21). TARE of hepatocellular carcinoma results in prolonged elevation of IL-10 (22) and infiltration of CD8+ TILs (6). In our study, TARE was associated with increased LAG3+ CD4+ TILs and nitric oxide synthase 2 expression and decreased mast cell levels. LAG3 expression is associated with PD-1 expression (23). LAG3+ TILs are associated with breast cancer–specific survival (24). Mast cells are found in high levels within solid tumors and modulate antitumor immunity (25), and nitric oxide signaling influences T-cell activation and helper T-cell differentiation (26). Taken together, findings suggest that TARE has immunomodulatory effects, in concordance with studies on external radiation (7,27). As a type of brachytherapy, TARE is expected to be more immunogenic than external radiation: brachytherapy delivers more heterogeneous and conformal dose distribution and is less antagonistic to peripheral immune cells (28). By delivering a high but “infinitely fractionated” radiation dose, TARE may be an optimal local-regional treatment to combine with immunotherapy (4,29).

More than a third of the participants in this study achieved CR, similar to retrospective studies of TARE for BCLM (2). Markers predicting response to TARE are elusive but could help exclude participants unlikely to benefit. Retrospective studies have suggested that PI3K pathway variations (3) and estrogen receptor positivity (30) may be potential predictors. In our study, PI3K pathway variation status was not associated with CR, although in the study by Deipolyi et al (3), allele status was correlated with objective response, rather than CR assessed herein. Our study also did not show a relationship between hormone receptor status and CR, although it was not designed to assess that.

Despite the small sample size, the results herein showed differences in baseline immune markers peripherally and in the tumor microenvironment between responders and nonresponders. The finding that peripheral immune markers may predict response is helpful given the ease of collecting blood. Low peripheral cytokine levels, MDSCs, and monocytes were associated with CR. MDSCs are immunosuppressive, and high levels in cancer are associated with poor prognosis and treatment resistance (31,32). The tumor microenvironment triggers the conversion of myeloid cells into MDSCs, which suppress CD8+ T cells, reducing antitumor immunity (31). IL-6 stimulates immunosuppressive MDSCs (33,34). Together, findings suggest that immunosuppression is associated with poor eventual response to TARE, concordant with observations that intact immunity is required for the antitumor effects of external radiation (5).

In our study, greater baseline PD-1 staining and PD-1+ CD4+ TILs in the tumor microenvironment were associated with response. The PD-1 pathway influences cytokine production and T-cell proliferation. Higher levels of PD-1+ CD4+ T cells are predictive of response to immune checkpoint inhibitors in lung cancer (35). These data suggest that PD-1 pathway agents may be potential immunotherapies to combine with TARE. Such strategies could augment possible beneficial effects of TARE in treating BCLM (4).

The primary study limitation is its small sample size. Imaging response was assessed at PET/CT because of its theoretical superiority for evaluating response in hypoenhancing tumors and its ability to help detect response earlier than with anatomic or enhancement-based criteria (2). However, the absence of more routine response criteria in our study limits its generalizability. Due to the complexity of the study design, not all participants were able to complete all study events. Therefore, specimens were not available for all analyses, possibly introducing unanticipated bias into the results. Given the number of tests, not all assays were feasible, including markers of interest such as cytotoxic T-lymphocyte–associated antigen 4. Many of the specimens were inadequate, further reducing numbers. Given that specialty serum markers are not routinely tested, the results presented here may not be generalized clinically. However, the findings from this hypothesis-generating pilot study suggest possible markers and targets that should be confirmed in future larger prospective studies.

In conclusion, transarterial radioembolization (TARE) performed for breast cancer liver metastasis induced inflammatory and immunogenic effects. Higher levels of cytokines and immunosuppressive peripheral myeloid-derived suppressor cells were associated with poorer response to TARE, suggesting that these may be useful prognostic markers. The finding that programmed cell death protein (PD) 1 levels in the tumor microenvironment were associated with response to TARE suggests the potential for combination therapy targeting the PD-1 and programmed death ligand 1 pathway to augment response to TARE.

Supplementary Material

Refer to Web version on PubMed Central for supplementary material.

Acknowledgments

A.R.D. supported by a Society of Interventional Radiology Foundation Pilot Research Grant, an RSNA Research & Education Foundation Research Seed Grant, and a Society of Memorial Sloan-Kettering Cancer Center Research Grant. Supported in part by the National Institutes of Health/National Cancer Institute Cancer Center Support Grant P30 CA008748.

Data sharing:

Data generated or analyzed during the study are available from the corresponding author by request.

Abbreviations

BCLM	breast cancer liver metastasis
CR	complete response
IL	interleukin
LAG3	lymphocyte activation gene 3
MDSC	myeloidderived suppressor cell

PD	programmed cell death protein
PI3K	phosphoinositide 3–kinase
SUV_{max}	maximum standardized uptake value
TARE	transarterial radioembolization
TIL	tumor-infiltrating lymphocyte

References

1. Liberchuk AN, Deipolyi AR. Hepatic metastasis from breast cancer. Semin Intervent Radiol 2020;37(5):518–526. [PubMed: 33328708]
2. Deipolyi AR, England RW, Ridouani F, et al. PET/CT imaging characteristics after radioembolization of hepatic metastasis from breast cancer. Cardiovasc Intervent Radiol 2020;43(3):488–494. [PubMed: 31732778]
3. Deipolyi AR, Riedl CC, Bromberg J, et al. Association of PI3K pathway mutations with early positron-emission tomography/CT imaging response after radioembolization for breast cancer liver metastases: results of a single-center retrospective pilot study. J Vasc Interv Radiol 2018;29(9):1226–1235. [PubMed: 30078647]
4. Deipolyi AR, Johnson CB, Erinjeri JP, Bryce YCD. Combination therapies with Y90: immunoradiation. Dig Dis Interv 2020;4(4):382–388.
5. Kalbasi A, June CH, Haas N, Vapiwala N. Radiation and immunotherapy: a synergistic combination. J Clin Invest 2013;123(7):2756–2763. [PubMed: 23863633]
6. Chew V, Lee YH, Pan L, et al. Immune activation underlies a sustained clinical response to yttrium-90 radioembolisation in hepatocellular carcinoma. Gut 2019;68(2):335–346. [PubMed: 29440463]
7. Burnette B, Weichselbaum RR. The immunology of ablative radiation. Semin Intervent Radiol 2015;25(1):40–45.
8. Kitano S, Postow MA, Ziegler CG, et al. Computational algorithm-driven evaluation of monocytic myeloid-derived suppressor cell frequency for prediction of clinical outcomes. Cancer Immunol Res 2014;2(8):812–821. [PubMed: 24844912]
9. Cheng DT, Mitchell TN, Zehir A, et al. Memorial Sloan Kettering-Integrated Mutation Profiling of Actionable Cancer Targets (MSK-IMPACT): a hybridization capture-based next-generation sequencing clinical assay for solid tumor molecular oncology. J Mol Diagn 2015;17(3):251–264. [PubMed: 25801821]
10. Salgado R, Denkert C, Demaria S, et al. The evaluation of tumor-infiltrating lymphocytes (TILs) in breast cancer: recommendations by an international TILs working group 2014. Ann Oncol 2015;26(2):259–271. [PubMed: 25214542]
11. Adams S, Loi S, Toppmeyer D, et al. Pembrolizumab monotherapy for previously untreated, PD-L1-positive, metastatic triple-negative breast cancer: cohort B of the phase II KEYNOTE-086 study. Ann Oncol 2019;30(3):405–411. [PubMed: 30475947]
12. Damotte D, Warren S, Arrondeau J, et al. The tumor inflammation signature (TIS) is associated with anti-PD-1 treatment benefit in the CERTIM pan-cancer cohort. J Transl Med 2019;17(1):357. [PubMed: 31684954]
13. Vadakekolathu J, Minden MD, Hood T, et al. Immune landscapes predict chemotherapy resistance and immunotherapy response in acute myeloid leukemia. Sci Transl Med 2020;12(546):eaaz0463. [PubMed: 32493790]
14. O JH, Lodge MA, Wahl RL. Practical PERCIST: a simplified guide to PET Response Criteria in Solid Tumors 1.0. Radiology 2016;280(2):576–584. [PubMed: 26909647]
15. Zerizer I, Al-Nahhas A, Towey D, et al. The role of early ^{18}F-FDG PET/CT in prediction of progression-free survival after ^{90}Y radioembolization: comparison with RECIST and tumour density criteria. Eur J Nucl Med Mol Imaging 2012;39(9):1391–1399. [PubMed: 22644713]

16. Fendler WP, Philippe Tiega DB, Ilhan H, et al. Validation of several SUV-based parameters derived from 18F-FDG PET for prediction of survival after SIRT of hepatic metastases from colorectal cancer. J Nucl Med 2013;54(8):1202–1208. [PubMed: 23729697]
17. Lynn HS. Maximum likelihood inference for left-censored HIV RNA data. Stat Med 2001;20(1):33–45. [PubMed: 11135346]
18. Erinjeri JP, Thomas CT, Samoilia A, et al. Image-guided thermal ablation of tumors increases the plasma level of interleukin-6 and interleukin-10. J Vasc Interv Radiol 2013;24(8):1105–1112. [PubMed: 23582441]
19. Cortes AC, Nishiofuku H, Polak U, et al. Effect of bead size and doxorubicin loading on tumor cellular injury after transarterial embolization and chemoembolization in a rat model of hepatocellular carcinoma. Nanomedicine (Lond) 2022;39:102465.
20. Doemel LA, Santana JG, Savic LJ, et al. Comparison of metabolic and immunologic responses to transarterial chemoembolization with different chemoembolic regimens in a rabbit VX2 liver tumor model. Eur Radiol 2022;32(4):2437–2447. [PubMed: 34718844]
21. Tischfield DJ, Gurevich A, Johnson O, et al. Transarterial embolization modulates the immune response within target and nontarget hepatocellular carcinomas in a rat model. Radiology 2022;303(1):215–225. [PubMed: 35014906]
22. Liu CA, Lee IC, Lee RC, et al. Prediction of survival according to kinetic changes of cytokines and hepatitis status following radioembolization with yttrium-90 microspheres. J Formos Med Assoc 2021;120(4):1127–1136. [PubMed: 32978044]
23. Solinas C, Migliori E, De Silva P, Willard-Gallo K. LAG3: the biological processes that motivate targeting this immune checkpoint molecule in human cancer. Cancers (Basel) 2019;11(8):1213. [PubMed: 31434339]
24. Burugu S, Gao D, Leung S, Chia SK, Nielsen TO. LAG-3+ tumor infiltrating lymphocytes in breast cancer: clinical correlates and association with PD-1/PD-L1+ tumors. Ann Oncol 2017;28(12):2977–2984. [PubMed: 29045526]
25. Oldford SA, Marshall JS. Mast cells as targets for immunotherapy of solid tumors. Mol Immunol 2015;63(1):113–124. [PubMed: 24698842]
26. García-Ortiz A, Serrador JM. Nitric oxide signaling in T cell-mediated immunity. Trends Mol Med 2018;24(4):412–427. [PubMed: 29519621]
27. Burnette B, Fu YX, Weichselbaum RR. The confluence of radiotherapy and immunotherapy. Front Oncol 2012;2:143. [PubMed: 23087904]
28. Patel RB, Baniel CC, Sriramaneni RN, Bradley K, Markovina S, Morris ZS. Combining brachytherapy and immunotherapy to achieve in situ tumor vaccination: a review of cooperative mechanisms and clinical opportunities. Brachytherapy 2018;17(6):995–1003. [Published correction appears in Brachytherapy 2019;18(2):240.] [PubMed: 30078541]
29. Fleischmann M, Glatzer M, Rödel C, Tselis N. Radioimmunotherapy: future prospects from the perspective of brachytherapy. J Contemp Brachytherapy 2021;13(4):458–467. [PubMed: 34484362]
30. Davisson NA, Bercu ZL, Friend SC, et al. Predictors of survival after yttrium-90 radioembolization of chemotherapy-refractory hepatic metastases from breast cancer. J Vasc Interv Radiol 2020;31(6):925–933. [PubMed: 32307310]
31. Gabrilovich DI, Ostrand-Rosenberg S, Bronte V. Coordinated regulation of myeloid cells by tumours. Nat Rev Immunol 2012;12(4):253–268. [PubMed: 22437938]
32. Shou D, Wen L, Song Z, Yin J, Sun Q, Gong W. Suppressive role of myeloid-derived suppressor cells (MDSCs) in the microenvironment of breast cancer and targeted immunotherapies. Oncotarget 2016;7(39):64505–64511. [PubMed: 27542274]
33. Jiang M, Chen J, Zhang W, et al. Interleukin-6 trans-signaling pathway promotes immunosuppressive myeloid-derived suppressor cells via suppression of suppressor of cytokine signaling 3 in breast cancer. Front Immunol 2017;8:1840. [PubMed: 29326716]
34. Yao X, Huang J, Zhong H, et al. Targeting interleukin-6 in inflammatory autoimmune diseases and cancers. Pharmacol Ther 2014;141(2):125–139. [PubMed: 24076269]

35. Inomata M, Kado T, Okazawa S, et al. Peripheral PD1-positive CD4 T-lymphocyte count can predict progression-free survival in patients with non-small cell lung cancer receiving immune checkpoint inhibitor. Anticancer Res 2019;39(12):6887–6893. [PubMed: 31810958]

Key Results

- In this prospective study of 20 women undergoing radioembolization of bilobar breast cancer liver metastasis, peripheral interleukin 10 (0.2 vs 0.4 pg/mL; $P = .001$) and intratumoral lymphocyte activation gene 3–positive CD4+ tumor-infiltrating lymphocytes (TILs) (15% vs 31%; $P < .001$) increased.
- Lower baseline peripheral myeloid-derived suppressor cells (1% vs 5%; $P < .001$) and higher intratumoral programmed cell death protein 1–positive CD4+ TILs (59% vs 26%; $P = .006$) were associated with complete response.

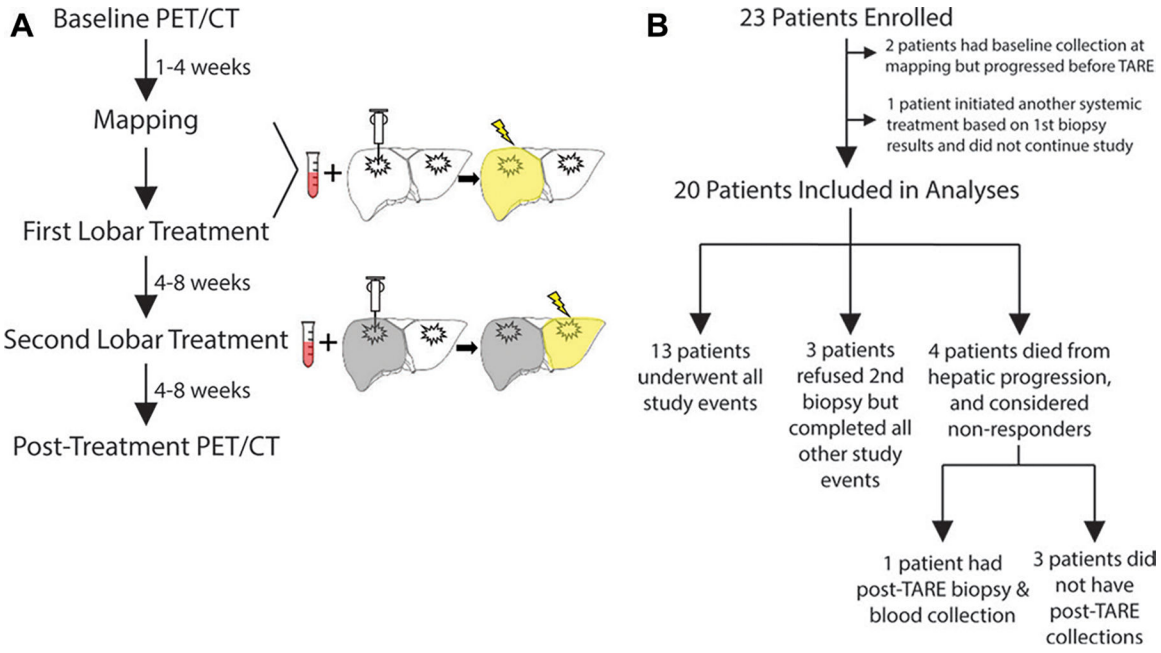

Figure 1:

Study schema. **(A)** Participants underwent a mapping procedure, two separate transarterial radioembolization (TARE) procedures, baseline and post-TARE blood collection and liver tumor biopsy, and PET/CT before and after TARE. **(B)** Of 23 participants initially enrolled, 20 were included in the study analyses. Three participants refused a second biopsy but underwent all other study events. Four participants died due to hepatic progression after the first TARE; of these, one underwent a post-TARE biopsy and blood collection during a paracentesis, while the other three had no follow-up tissue collection.

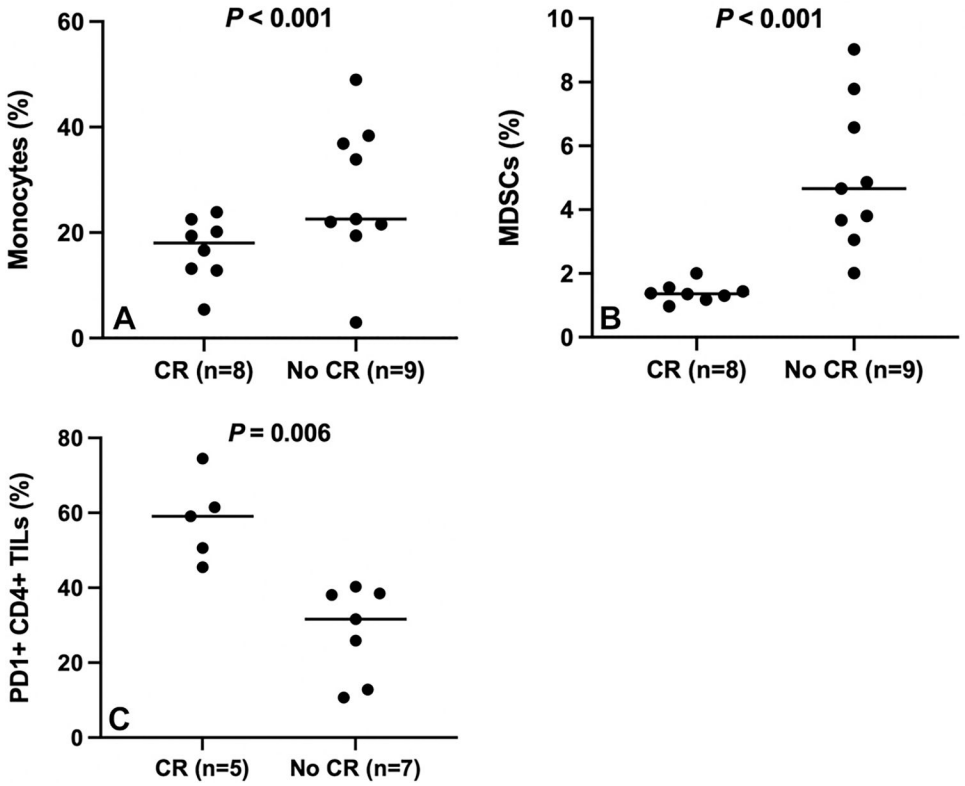

Figure 2:

Baseline immune cell levels by response status. Plots show **(A)** monocyte, **(B)** myeloid-derived suppressor cell (MDSC), and **(C)** programmed cell death protein 1 (PD1)–positive CD4+ tumor-infiltrating lymphocyte (TIL) values by response status. The horizontal lines represent the means. CR = complete response.

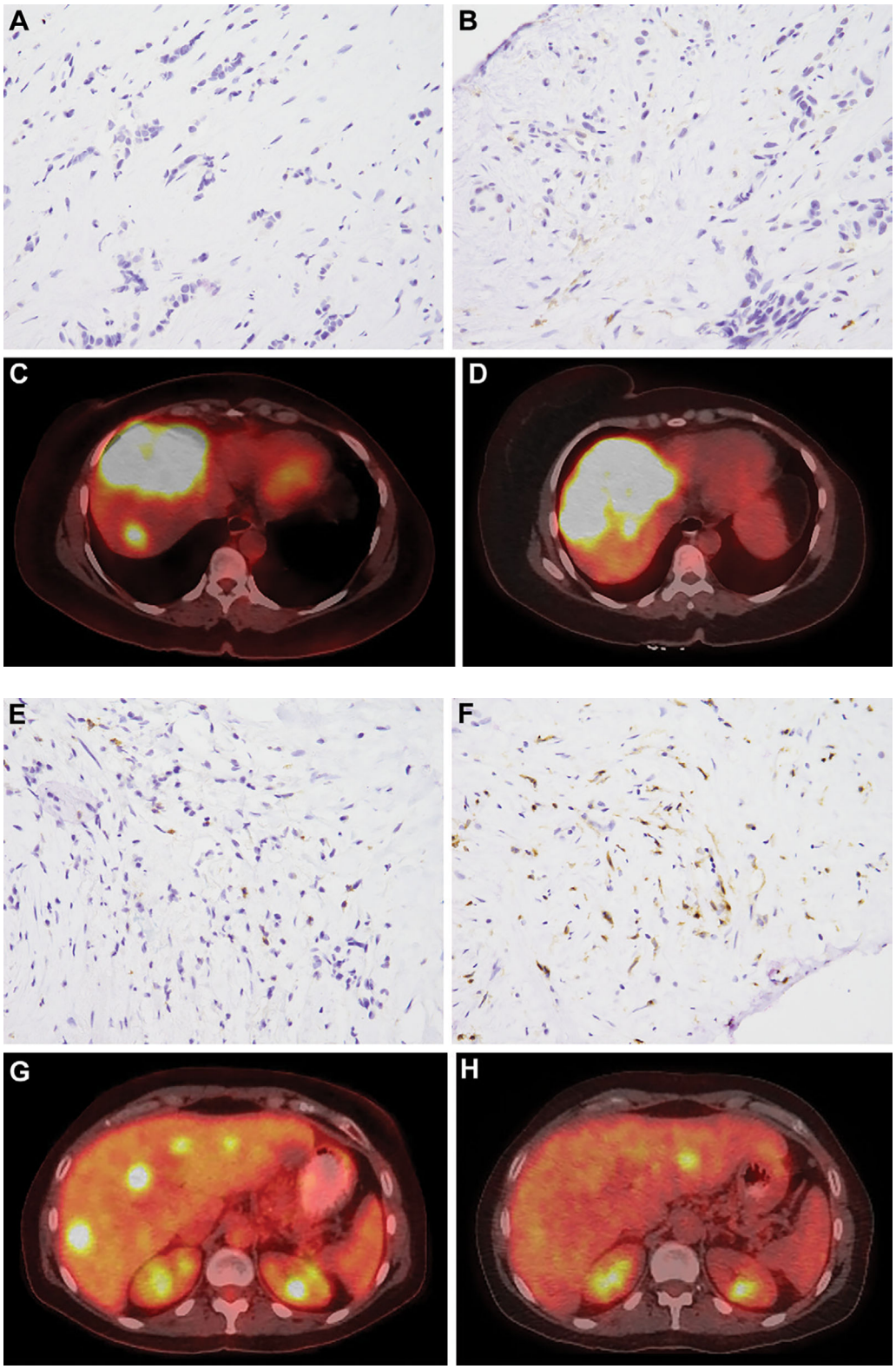

Figure 3:

A 47-year-old woman with metastatic breast cancer underwent transarterial radioembolization (TARE), with the first treatment to the right lobe of the liver. Pre-TARE baseline biopsy specimens show **(A)** low programmed cell death protein (PD) 1 staining (DAB brown) and **(B)** low CD4 staining (brown) (magnification, ×400). PET/CT images **(C)** before and **(D)** after TARE demonstrate progressive disease. A 51-year-old woman with metastatic breast cancer underwent TARE, with the first treatment to the right lobe of the liver. Pre-TARE baseline biopsy specimens show **(E)** high PD-1 staining and **(F)** high CD4 staining (magnification, ×400). PET/CT images **(G)** before and **(H)** after TARE demonstrate complete response.

Table 1:

Participant Characteristics

Characteristic	Complete Responders (*n* = 8)	Nonresponders (*n* = 12)	*P* Value
Age (y) *	61 (56–69)	53 (46–61)	.10
Hormone receptor status			
Estrogen receptor–positive	7 (88)	11 (92)	>.99
Progesterone receptor–positive	5 (62)	8 (67)	>.99
Human epidermal growth factor receptor 2–positive	0 (0)	2 (17)	.49
Systemic therapy			
≤30 days before TARE			
None	2 (25)	0 (0)	.15
Fulvestrant	1	3	.62
Eribulin	1	1	>.99
Paclitaxel	1	1	>.99
Doxorubicin	1	1	>.99
Irinotecan	1	0	.40
Capecitabine	1	0	.40
Dexrazoxane	1	0	.40
Denosumab	0	4	.12
Gemcitabine	0	2	.49
Investigational agent	0	1	>.99
Vinorelbine	0	1	>.99
Ribociclib	0	1	>.99
Trastuzumab	0	2	.49
Pre-TARE imaging			
CT with contrast enhancement	7 (88)	8 (67)	.60
MRI with contrast enhancement	0 (0)	2 (17)	.49
PET/CT	8 (100)	12 (100)	>.99
Tumor burden (%) *	7 (4–20)	25 (16–41)	.054
Pre-TARE SUV_{max} *	8 (5–10)	9 (7–12)	.79
No. of tumors *	5 (4–8)	5 (4–7)	.78
Hypoenhancing tumors	7/7 (100)	10/10 (100)	>.99
Lung shunt fraction (%) *	4 (3–5)	4 (3–5)	.88
Yttrium 90 activity (MBq) *	2812 (2294–2997)	3034 (2627–4736)	.19
Neutrophil-to-lymphocyte ratio *	1.9 (1.5–2.9)	4.5 (2.6–6.3)	.01

Note.—Unless otherwise specified, data are numbers of participants, with percentages in parentheses. Groups of continuous data were compared by using Wilcoxon rank-sum tests. Categorical data were analyzed with Fisher exact tests. SUV_{max} = maximum standardized uptake value, TARE = transarterial radioembolization.

* Data are medians, with IQRs in parentheses.

Table 2:

Inclusion and Exclusion Criteria

Inclusion Criteria	Exclusion Criteria
Diagnosis of bilobar hepatic disease with plan to undergo two separate lobar yttrium 90 infusions	Eastern Cooperative Oncology Group performance status of 2 or greater
Not pregnant	Tumor replacement >70% of liver
Age 18 years and older	Creatinine >2 mg/dL
Any racial or ethnic group	Bilirubin >1.2 times the upper limit of normal
Ineligible for thermal ablation or surgical resection	Albumin <2 g/dL

Table 3:

Changes in Immune Markers after TARE

Cytometry Type and Marker	Pre-TARE Level	Post-TARE Level	Relative Difference	*P* Value
Peripheral blood flow cytometry				
No. of participants	17	17		
IL-10 (pg/mL)	0.2 (1.7)	0.4 (2.0)	1.9 (1.4, 2.7)	.001
IL-6 (pg/mL)	1.0 (3.8)	1.6 (3.8)	1.6 (1.1, 2.4)	.02
IL-8 (pg/mL)	13.5 (3.7)	15.6 (3.9)	1.2 (0.9, 1.5)	.30
IL-15 (pg/mL)	1.9 (1.7)	2.4 (1.5)	1.3 (1.1, 1.6)	.01
Monocytes (%)	18 (2)	20 (2)	1 (1, 2)	.81
Myeloid-derived suppressor cells (%)	3 (2)	3 (2)	1 (1, 2)	.64
Tumor biopsy flow cytometry				
No. of participants	12	12		
CD3+ CD8+ TIL (%)	42 (1)	29 (2)	1 (0, 1)	.09
CD3+ CD4+ TIL (%)	30 (2)	35 (1)	1 (1, 2)	.43
PD-1 + CD8+ TIL (%)	47 (1)	32 (3)	1 (0, 1)	.31
PD-1 + CD4+ TIL (%)	37 (2)	27 (2)	1 (0, 1)	.11
Tim3+ CD8+ TIL (%)	3 (2)	4 (3)	1 (1, 2)	.24
Tim3+ CD4+ TIL (%)	3 (2)	2 (2)	1 (0, 1)	.34
CD8+/CD4+ regulatory T cell	16.0 (2.5)	11.5 (2.2)	0.7 (0.3, 1.6)	.36
CTLA4+ CD8+ TIL (%)	2 (2)	1 (2)	1 (1, 1)	.53
LAG 3+ CD4+ TIL (%)	15 (3)	31 (3)	2 (1, 3)	<.001
iCOS+ CD4+ TIL (%)	6 (2)	5 (2)	1 (0, 2)	.50

Note.—Marker values are geometric means, with geometric SD factors in parentheses. Differences are defined as post-TARE value divided by pre-TARE value and are shown with 95% CIs in parentheses. Log-transformed pre- and post-TARE values were compared using paired *t* tests. CTLA4 = cytotoxic T-lymphocyte–associated antigen 4, iCOS = inducible T-cell costimulator, IL = interleukin, LAG3 = lymphocyte activation gene 3, PD-1 = programmed cell death protein 1, TARE = transarterial radioembolization, TIL = tumor-infiltrating lymphocyte, Tim3 = T cell immunoglobulin and mucin domain 3.

Table 4:

Comparison of Responders′ and Nonresponders′ Baseline Immune Markers

Cytometry Type and Marker	Complete Responders	Nonresponders	*P* Value
Peripheral blood flow cytometry			
No. of participants	8	9	
IL-10 (pg/mL)	0.2 (0.1, 0.9)	0.3 (0.2, 0.4)	.04
IL-6 (pg/mL)	0.5 (0.2, 1.2)	1.8 (0.7, 4.6)	.04
IL-8 (pg/mL)	9.4 (3.5, 25.5)	18.7 (6.4, 55.2)	.29
IL-15 (pg/mL)	1.8 (1.4, 2.3)	1.9 (1.1, 3.2)	>.99
Monocytes (%)	10 (8, 14)	29 (23, 36)	<.001
Myeloid-derived suppressor cells (%)	1 (1, 2)	5 (3, 7)	<.001
Tumor biopsy tissue flow cytometry			
No. of participants	5	7	
CD8+ TIL (%)	38 (25, 58)	45 (35, 58)	.36
CD4+ TIL (%)	33 (25, 43)	28 (17, 45)	.43
PD-1 + CD8+ TIL (%)	53 (43, 65)	43 (29, 65)	.29
PD-1 + CD4+ TIL (%)	59 (47, 74)	26 (16, 43)	.006
Tim3+ CD8+ TIL (%)	3 (1, 12)	2 (1, 5)	.54
Tim3+ CD4+ TIL (%)	4 (2, 9)	2 (1, 5)	.15
CD8+/CD4+ regulatory T cell	10.8 (3.3, 35.9)	21.1 (10.1, 44.3)	.24
CTLA4+ CD8+ TIL (%)	2 (1, 5)	1 (1, 2)	.53
LAG3+ CD4+ TIL (%)	18 (6, 56)	13 (5, 35)	.59
iCOS+ CD4+ TIL (%)	9 (3, 32)	4 (3, 6)	.17
Tumor biopsy tissue: PD-1/PD-L1 IHC			
No. of participants	8	6	
PD-1 staining (%)*	2 (1–2)	1 (0–1)	.046
PD-L1 staining (%)*	0 (0–1)	0 (0–1)	.95
Tumor biopsy tissue: other IHC			
No. of participants	6	5	
CD4+ staining (%)*	8 (5–14)	2 (1–5)	.19
CD8+ staining (%)*	10 (4–10)	2 (1–2)	.11
CD14+ staining (%)*	10 (6–18)	25 (10–30)	.31
LAG3+ staining (%)*	1 (1–1)	1 (0–1)	.48

Note.—Unless otherwise specified, data are geometric means, with 95% CIs in parentheses. Groups were compared on the natural logarithmic scale with use of Welch two-sample *t* tests. CTLA4 = cytotoxic T-lymphocyte–associated antigen 4, IHC = immunohistochemistry, iCOS = inducible T cell costimulator, IL = interleukin, LAG3 = lymphocyte activation gene 3, PD-1 = programmed cell death protein 1, PD-L1 = programmed death ligand 1, TARE = transarterial radioembolization, TIL = tumor- infiltrating lymphocyte, Tim3 = T cell immunoglobulin and mucin domain 3.

*Due to the small number of available data, IHC staining data are summarized as medians with IQRs and were compared between groups with use of the Wilcoxon rank-sum test.